Reflection and transmission of Laguerre Gaussian beam from uniaxial anisotropic multilayered media*

Hai-Ying Li(李海英)[1,2,†], Zhen-Sen Wu(吴振森)[1,2], Qing-Chao Shang(尚庆超)[1], Lu Bai(白璐)[1,2], and Zheng-Jun Li(李正军)[1]

[1] School of Physics and Optoelectronic Engineering, Xidian University, Xi'an 710071, China
[2] Collaborative Innovation Center of Information Sensing and Understanding at Xidian University, Xi'an 710071, China

(Received 3 November 2016; revised manuscript received 24 November 2016; published online 13 February 2017)

Based on angular spectrum expansion and 4×4 matrix theory, the reflection and transmission characteristics of a Laguerre Gaussian (LG) beam from uniaxial anisotropic multilayered media are studied. The reflected and transmitted beam fields of an LG beam are derived. In the case where the principal coordinates of the uniaxial anisotropic media coincide with the global coordinates, the reflected and transmitted beam intensities from a uniaxial anisotropic slab and three-layered media are numerically simulated. It is shown that the reflected intensity components of the incident beam, especially the TM polarized incident beam, are smaller than the transmitted intensity components. The distortion of the reflected intensity component is more evident than that of the transmitted intensity component. The distortion of intensity distribution is greatly affected by the dielectric tensor and the thickness of anisotropic media. We finally extend the application of the method to general anisotropic multilayered media.

Keywords: Laguerre Gaussian beam, reflection and transmission, uniaxial anisotropic multilayered media

PACS: 42.25.Bs, 42.60.Jf, 42.25.Gy **DOI:** 10.1088/1674-1056/26/3/034204

1. Introduction

Since the Laguerre Gaussian (LG) vortex beam was demonstrated to possess orbital angular momentum (OAM),[1] light vortex beams carrying OAM have been attracting great attention of many scholars. This kind of beam has vast potential applications in the fields of optical manipulation,[2] quantum and optical information,[3,4] optical detection,[5] object recognition,[6] marine remote sensing,[7,8] etc. Extensive research results[9–18] addressing the generation methods, propagation characteristics and applications of the OAM light beams have been presented in recent decades. LG beams are recognized as the typical vortex beams.

As is well known, the propagation of beams in different media is an important research topic. With the increases of applications of anisotropic media in the optical signal processing, the optical fiber designing, and the radar cross section controlling, the interaction between anisotropic media and beam, especially the reflection and transmission of Gaussian beam at an isotropic–uniaxial interface,[19] uniaxial slabs,[20–23] and anisotropic multilayer structures[24,25] have been intensively investigated. For an LG beam, its reflection and transmission characteristics at a dielectric interface,[26,27] as well as its propagations in a uniaxial crystal,[28–30] the nonlinear media,[31,32] and the left-handed materials[33] are also studied in detail. However, if the anisotropic media are inhomogeneous, the propagation properties of LG beam have not been reported yet. Research on the effects of anisotropic media on beam distortion may be applied to birefringent filter design, thin-film analysis, ellipsometry, etc. Therefore, our goal here is to study the reflection and transmission of LG beam from uniaxial anisotropic multilayered media in which the input and output regions are isotropic and have their own refraction indices.

In order to use the relevant formula of plane wave in the reflection and transmission of beam, the plane angular spectrum expansion method is always one of the best choices. For the investigation of isotropic–isotropic interface and isotropic multilayer medium, Snell's law, Fresnel coefficient, generalized Fresnel coefficient of plane wave, and one-dimensional angular spectrum expansion are used. Meanwhile, the 4×4 matrix theory of plane wave which was presented by Berreman,[34] and refined by other authors[35,36] is usually used in both isotropic and anisotropic multilayered media. However, considering the dielectric properties of the anisotropic media, the two-dimensional angular spectrum expansion and corresponding extended 4×4 matrix theory should be employed here.

In this work, the reflection and transmission characteristics of an LG beam from uniaxial anisotropic multilayered media are analyzed on the basis of angular spectrum expansion and 4×4 matrix theory. The reflected and transmitted

*Project supported by the National Natural Science Foundation of China (Grant Nos. 61475123, 61571355, and 61308025), the Natural Science Basic Research Plan in Shaanxi Province, China (Grant No. 2016JQ4015), and the Overseas Training Program for Young Backbones Teachers Sponsored by China Scholarship Council and Xidian University.

†Corresponding author. E-mail: lihy@xidian.edu.cn

© 2017 Chinese Physical Society and IOP Publishing Ltd

electric field expressions from uniaxial anisotropic media are presented in Section 2. The numerical results on the distribution of the reflected and transmitted beam intensities from a uniaxial slab and three-layered uniaxial anisotropic media, a comparison between the intensities of both TE and TM polarized LG beams, as well as a discussion on the applicability of this method in general anisotropic media are provided in Section 3. In Section 4 the main conclusions are drawn from the present studies.

2. Reflected and transmitted fields of LG beam from uniaxial anisotropic media

Considering an arbitrary linearly polarized LG beam incident on the interface of the uniaxial anisotropic N-layered media, the locations of global and local coordinates are shown in Fig. 1. The x_α–y_α planes in the local coordinates $(x_\alpha, y_\alpha, z_\alpha)$, $\alpha =$ i, r or t represent the transverse planes of the incident, reflected and transmitted beams, respectively. The positive direction of y_α axis is perpendicular to the surface outward, and θ_i denotes the incident angle. The reflection and transmission output planes are described by the angles θ_r and θ_t.

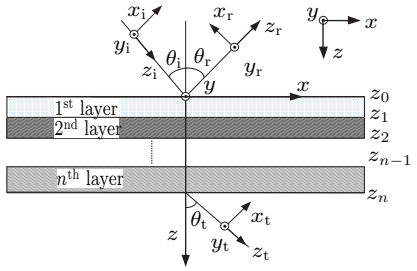


Fig. 1. Schematic of Laguerre Gaussian beam incident on uniaxial anisotropic N-multilayered media.

The input and the output regions are both assumed to be isotropic, and their dielectric constants are ε_i and ε_t, respectively. Providing that the principal coordinates of uniaxial anisotropic media are coincident with the global coordinates (x, y, z), the dielectric tensor $\boldsymbol{\varepsilon}_j$ of the j^{th} layer is

$$\boldsymbol{\varepsilon}_j = \begin{bmatrix} \varepsilon_{x,j} & 0 & 0 \\ 0 & \varepsilon_{x,j} & 0 \\ 0 & 0 & \varepsilon_{z,j} \end{bmatrix}. \tag{1}$$

The complex electric field amplitude of the TE or TM polarized LG beam in the incident coordinate system is represented as follows:

$$E_\mathrm{i}(r_\mathrm{i}, \phi_\mathrm{i}, z_\mathrm{i}=0) = E_0 \left[\frac{\sqrt{2}r_\mathrm{i}}{w_0}\right]^{|l|} \exp\left[\frac{-r_\mathrm{i}^2}{w_0^2}\right] L_p^{|l|}\left(\frac{2r_\mathrm{i}^2}{w_0^2}\right) \times \exp(\mathrm{i}l\phi_\mathrm{i}), \tag{2}$$

where $E_0 = \sqrt{2p!/\pi(p+|l|)!}/w_0$ is the amplitude constant, w_0 is the beam waist radius at $z_\mathrm{i}=0$, $r_\mathrm{i} = \sqrt{x_\mathrm{i}^2+y_\mathrm{i}^2}$, $\phi_\mathrm{i} = \mathrm{atan}(y_\mathrm{i}/x_\mathrm{i})$, $L_p^{|l|}(\cdot)$ is the associated Laguerre polynomial, p and l represent the radial index and the topological charge of the LG mode, respectively. The time dependence factor of $\exp(-\mathrm{i}\omega t)$ is omitted.

By using the plane angular spectrum expansion, the complex amplitude function $\bar{E}(k_\mathrm{i}, \varphi_\mathrm{i})$ can be obtained by the two-dimensional forward Fourier transform of Eq. (2) and be expressed as[26]

$$\bar{E}_\mathrm{i}(k_\mathrm{i}, \varphi_\mathrm{i}) = E_0 \mathrm{i}^l \exp(\mathrm{i}l\varphi_\mathrm{i}) \left(\frac{w_0}{\sqrt{2}}\right)^2 (-1)^{p+1} \left(\frac{k_\mathrm{i}}{\sqrt{2}k_0 f}\right)^l \times \exp\left(-\frac{k_\mathrm{i}^2}{4k_0^2 f^2}\right) L_p^{|l|}\left(\frac{k_\mathrm{i}^2}{2k_0^2 f^2}\right), \tag{3}$$

where k_i is the transverse component of the wave vector $\boldsymbol{k}$ in the incident coordinates, $\phi_\mathrm{i} = \mathrm{atan}(k_{y\mathrm{i}}/k_{x\mathrm{i}})$, $k_0 = |\boldsymbol{k}|$ is the wave number of the LG beam, and $f = 1/k_0 w_0$ is the natural expansion factor appearing in Ref. [37]. Using the inverse Fourier transform, the input field is written as

$$E_\mathrm{i}(r_\mathrm{i}, \phi_\mathrm{i}, z_\mathrm{i}=0) = \frac{1}{2\pi}\int_0^\infty \int_0^{2\pi} \bar{E}_\mathrm{i}(k_\mathrm{i}, \varphi_\mathrm{i}) \times \exp[\mathrm{i}k_\mathrm{i} r_\mathrm{i}\cos(\phi_\mathrm{i}-\varphi_\mathrm{i})] k_\mathrm{i}\,\mathrm{d}k_\mathrm{i}\,\mathrm{d}\varphi_\mathrm{i}. \tag{4}$$

Meanwhile, the electric fields in the reflected and transmitted output planes can also be written as

$$\begin{aligned} &E_\mathrm{r}(r_\mathrm{r}, \phi_\mathrm{r}, z_\mathrm{r}=0) \\ &= \frac{1}{2\pi}\int_0^\infty \int_0^{2\pi} r(k_x, k_y)\bar{E}_\mathrm{i}(k_\mathrm{i}, \varphi_\mathrm{i}) \exp[\mathrm{i}k_\mathrm{r} r_\mathrm{r}\cos(\phi_\mathrm{r}-\varphi_\mathrm{r})] \\ &\quad \times \exp[\mathrm{i}k_{z\mathrm{r}}(z_1+z_2)] k_\mathrm{r}\,\mathrm{d}k_\mathrm{r}\,\mathrm{d}\varphi_\mathrm{r}, \end{aligned} \tag{5}$$

$$\begin{aligned} &E_\mathrm{t}(r_\mathrm{t}, \phi_\mathrm{t}, z_\mathrm{t}=0) \\ &= \frac{1}{2\pi}\int_0^\infty \int_0^{2\pi} t(k_x, k_y)\bar{E}_\mathrm{i}(k_\mathrm{i}, \varphi_\mathrm{i}) \exp[\mathrm{i}k_\mathrm{t} r_\mathrm{t}\cos(\phi_\mathrm{t}-\varphi_\mathrm{t})] \\ &\quad \times \exp[\mathrm{i}(k_{z\mathrm{i}}z_1 + k_{z\mathrm{t}}z_3)] k_\mathrm{t}\,\mathrm{d}k_\mathrm{t}\,\mathrm{d}\varphi_\mathrm{t}. \end{aligned} \tag{6}$$

Here $r_\mathrm{r} = \sqrt{x_\mathrm{r}^2+y_\mathrm{r}^2}$, $\phi_\mathrm{r} = \mathrm{atan}(y_\mathrm{r}/x_\mathrm{r})$, $r_\mathrm{t} = \sqrt{x_\mathrm{t}^2+y_\mathrm{t}^2}$, $\phi_\mathrm{t} = \mathrm{atan}(y_\mathrm{t}/x_\mathrm{t})$, $\varphi_\mathrm{r} = \mathrm{atan}(k_{y\mathrm{r}}/k_{x\mathrm{r}})$, $\varphi_\mathrm{t} = \mathrm{atan}(k_{y\mathrm{t}}/k_{x\mathrm{t}})$, $r(k_x, k_y)$, and $t(k_x, k_y)$ are the total reflected and transmitted coefficients of the multilayered anisotropic media, respectively. It should be noticed that the two coefficients are defined in the global coordinates. The k_r and k_t are the transverse components of the wave vector in the reflected and transmitted coordinates. The $k_{z\mathrm{i}}$, $k_{z\mathrm{r}}$ and $k_{z\mathrm{t}}$ are the longitudinal components of the wave vector in the local coordinates $(x_\alpha, y_\alpha, z_\alpha)$. The z_1, z_2, and z_3 are the distances between the center of the global coordinates and the centers of the incident coordinates, the reflected coordinates, and the transmitted coordinates.

Based on the 4×4 matrix theory, the transfer matrix $\boldsymbol{P}_j(h_j)$ of the j^{th} layer which describes the propagation of plane wave in the uniaxial anisotropic media, indicates that the relationship between the transverse field components $\boldsymbol{\psi}^j(z_{j-1})$ and $\boldsymbol{\psi}^j(z_{j-1}+h_j)$ has the following expression:[35]

$$\boldsymbol{P}_j(h_j) = \beta_0 \boldsymbol{I} - \beta_1 \boldsymbol{\Delta}_j + \beta_2 \boldsymbol{\Delta}_j^2 - \beta_3 \boldsymbol{\Delta}_j^3. \tag{7}$$

The scalars β_j $(j=0,1,2,3)$ are determined by the expanded equations of $\exp(\mathrm{i}k_0\tilde{k}_{zm,j}h_j)$, where h_j is the thickness of the j^{th} layer. $\boldsymbol{I}$ is a 4×4 unit matrix. $\tilde{k}_{zm,j}=k_{zm,j}/k_0(m=1,2,3,4)$ represent the normalized longitudinal wave vector components and are expressed as[34]

$$\tilde{k}_{z_{2,j}^1}=\pm\left[a_1-\left(a_1^2-a_2\right)^{1/2}\right]^{1/2},$$
$$\tilde{k}_{z_{4,j}^3}=\pm\left[a_1+\left(a_1^2-a_2\right)^{1/2}\right]^{1/2}, \tag{8}$$

where

$$a_1=-\frac{\left(\tilde{\varepsilon}_{x,j}+\tilde{\varepsilon}_{z,j}\right)\left(\tilde{k}_{x,j}^2+\tilde{k}_{y,j}^2\right)}{2\tilde{\varepsilon}_{z,j}}+\tilde{\varepsilon}_{x,j},\quad a_2=\frac{\tilde{\varepsilon}_{x,j}\left(\tilde{k}_{x,j}^4+\tilde{k}_{y,j}^4\right)+2\tilde{k}_{x,j}^2\tilde{k}_{y,j}^2\tilde{\varepsilon}_{x,j}-\left(\tilde{k}_{x,j}^2+\tilde{k}_{y,j}^2\right)\tilde{\varepsilon}_{x,j}\left(\tilde{\varepsilon}_{x,j}+\tilde{\varepsilon}_{z,j}\right)}{\tilde{\varepsilon}_{z,j}}+\tilde{\varepsilon}_{x,j}^2. \tag{9}$$

Substituting Eq. (1) into the differential expressions of Maxwell equations, the matrix $\boldsymbol{\Delta}_j$ in the j^{th} layer is deduced and written as

$$\boldsymbol{\Delta}_j=\begin{bmatrix}0 & 1-\dfrac{\tilde{k}_{x,j}^2}{\tilde{\varepsilon}_{z,j}} & 0 & \dfrac{\tilde{k}_{x,j}\tilde{k}_{y,j}}{\tilde{\varepsilon}_{z,j}}\\ \tilde{\varepsilon}_{x,j}-\tilde{k}_{y,j}^2 & 0 & \tilde{k}_{x,j}\tilde{k}_{y,j} & 0\\ 0 & -\dfrac{\tilde{k}_{x,j}\tilde{k}_{y,j}}{\tilde{\varepsilon}_{z,j}} & 0 & \dfrac{\tilde{k}_{y,j}^2}{\tilde{\varepsilon}_{z,j}}-1\\ -\tilde{k}_{x,j}\tilde{k}_{y,j} & 0 & \tilde{k}_{x,j}^2-\tilde{\varepsilon}_{x,j} & 0\end{bmatrix}, \tag{10}$$

where $\tilde{k}_{x,j}=k_{x,j}/k_0$, $\tilde{k}_{y,j}=k_{y,j}/k_0$, $\tilde{\varepsilon}_{z,j}=\varepsilon_{z,j}/\varepsilon_0$, $\tilde{\varepsilon}_{x,j}=\varepsilon_{x,j}/\varepsilon_0$, and ε_0 is the dielectric constant in vacuum.

In the input and output interfaces, the entrance and exit tangential field components are linked by the coefficient matrix as follows:[24]

$$\boldsymbol{\Psi}_\gamma=\begin{bmatrix}\cos(\theta_\gamma) & -\cos(\theta_\gamma) & 0 & 0\\ \sqrt{\varepsilon_\gamma/\varepsilon_0} & \sqrt{\varepsilon_\gamma/\varepsilon_0} & 0 & 0\\ 0 & 0 & 1 & 1\\ 0 & 0 & -\sqrt{\varepsilon_\gamma/\varepsilon_0}\cos(\theta_\gamma) & \sqrt{\varepsilon_\gamma/\varepsilon_0}\cos(\theta_\gamma)\end{bmatrix},\quad \gamma=\mathrm{i}\ \ \text{or}\ \ \mathrm{t}. \tag{11}$$

Therefore, for the uniaxial anisotropic N-layered media, the incident, reflected, and transmitted fields can be related by[34]

$$\boldsymbol{T}=\boldsymbol{\Psi}_{\mathrm{t}}^{-1}\left[\prod_{j=1}^{N}\boldsymbol{P}_j(h_j)\right]\boldsymbol{\Psi}_{\mathrm{i}}. \tag{12}$$

The matrix $\boldsymbol{T}$ represents the propagation characteristics of the uniaxial N-layered media. The total reflected and transmitted coefficients $r(k_x,k_y)$ and $t(k_x,k_y)$ are expressed by the elements of the matrix $\boldsymbol{T}$. Substituting the reflected and transmitted coefficients into Eqs. (5) and (6), the integrals can be evaluated by the two-dimensional midpoint rule.

3. Numerical results and discussion

3.1. Reflected and transmitted beam intensities from uniaxial anisotropic media

By using the theory presented in Section 2, the reflection and transmission characteristics of an LG beam from uniaxial anisotropic media are given in this section. In the simulation, the beam waist radius is 1000λ, the incident angle is 30°, z_1, z_2, and z_3 are all set to be 10 cm.

When an LG beam is incident on a uniaxial anisotropic slab, numerical results of the reflected and transmitted beam intensities are shown in Figs. 2–4, respectively. Each figure includes 4 panels. Panels (a) and (c) represent the case of a TE polarized incident beam; panels (b) and (d) correspond to the results of a TM polarized incident beam. For Figs. 2 and 3, the wavelength of incident beam is $\lambda=0.6328$ μm, which is radiated from a He–Ne laser. The elements of dielectric tensor for a calcite slab are $\tilde{\varepsilon}_x=2.744$ and $\tilde{\varepsilon}_z=2.207$, and the thickness of the slab is $h=0.2$ mm.

In Fig. 2, the radial index and the topological charge of the LG beam are $p=0$ and $l=1$, respectively. It is illustrated in Fig. 2 that the reflected intensities of a TE polarized LG beam and the transmitted intensities for both polarization modes have similar contours to that of the incident LG beam, whereas the intensity distribution is distorted and no longer circularly symmetric. The reflected intensities of a TM polarized incident beam in Fig. 2(b) are smaller and the distortion of its counter is more notable than those in Fig. 2(a). Regarding the two polarization modes of the incident beams, the intensity of transmitted beam is larger than that of the reflected beam, and most of the intensity transmits through the slab.

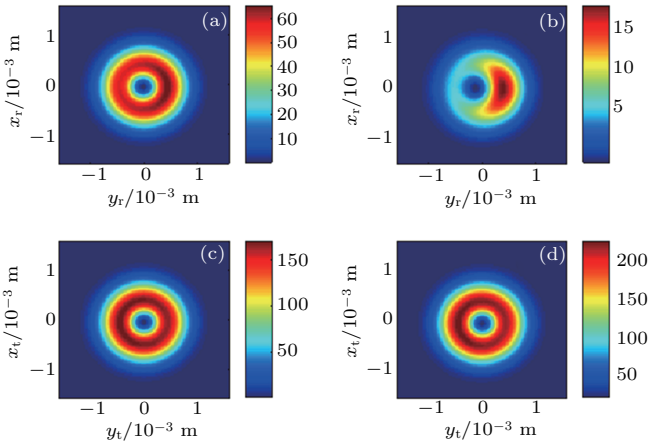


Fig. 2. (color online) Reflected and transmitted beam intensities of LG ($p = 0, l = 1$) beams incident on a uniaxial anisotropic slab, showing (a) reflected beam intensities (TE polarized LG beam), (b) reflected beam intensities (TM polarized LG beam), (c) transmitted beam intensities (TE polarized LG beam), and (d) transmitted beam intensities (TM polarized LG beam).

In Fig. 3, except the radial index $p = 1$ of the incident beam, other parameters are kept the same as those of Fig. 2. A comparison between Fig. 3 and Fig. 2 indicates that as the radial index of the incident beam varies from 0 to 1, the contour of intensity distribution increases a concentric circle, just like the shape of the incident LG beam. Other features of intensity distribution in Fig. 3 are similar to those in Fig. 2.

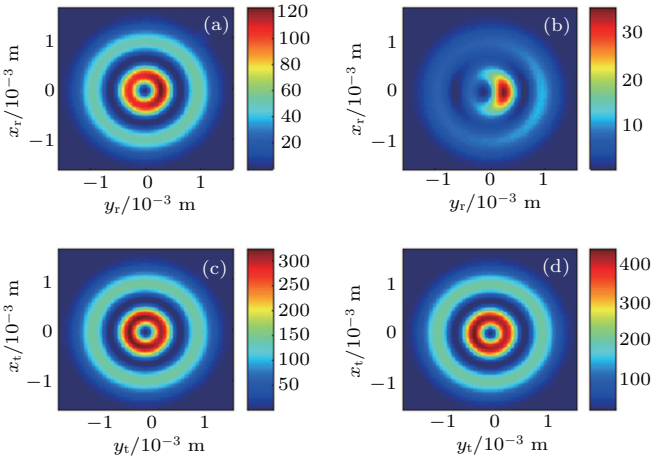


Fig. 3. (color online) Reflected and transmitted beam intensities of LG ($p = 1, l = 1$) beams incident on a uniaxial anisotropic slab, showing (a) reflected beam intensities (TE polarized LG beam), (b) reflected beam intensities (TM polarized LG beam), (c) transmitted beam intensities (TE polarized LG beam), and (d) transmitted beam intensities (TM polarized LG beam).

In order to analyze the effects of both the beam and the slab parameters on the distribution of intensities, the results are given in Fig. 4, with the parameters set to be $\lambda = 0.5893$ μm (which is radiated from a yellow laser), $h = 0.2$ mm, $\tilde{\varepsilon}_x = 2.7502$, and $\tilde{\varepsilon}_z = 2.2094$.

In Fig. 4, because of the changes of dielectric tensor and the incident wavelength, the distortions of the reflected intensities for both polarization modes and the transmitted intensities for the TE polarized incident LG beam are more visible than the results of Fig. 2, and the contour of the reflected intensity for a TM polarized incident beam does not keep a circular shape.

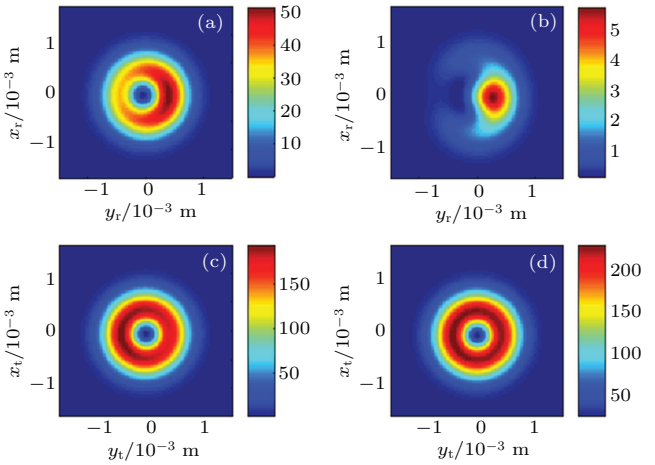


Fig. 4. (color online) Reflected and transmitted beam intensities of LG ($p = 0, l = 1$) beams incident on a uniaxial anisotropic slab, showing (a) reflected beam intensities (TE polarized LG beam), (b) reflected beam intensities (TM polarized LG beam), (c) transmitted beam intensities (TE polarized LG beam), and (d) transmitted beam intensities (TM polarized LG beam).

In general, the combination of all the results of Figs. 2–4, shows that the reflected intensity of an LG beam from the uniaxial slab is smaller than the corresponding transmitted result, especially for the intensity of the TM polarized incident beam.

To verify the practicability of the method in the analysis of LG beam propagation in uniaxial anisotropic multilayered media, figure 5 presents the reflected and transmitted intensities of LG beams from three-layered media. The wavelength of the incident beam is $\lambda = 0.5893$ μm. The thickness values and dielectric tensors are given in Table 1.

Table 1. Thickness values and dielectric tensors of the three-layered media.

Layer	$\tilde{\varepsilon}_x$	$\tilde{\varepsilon}_z$	h
1 (Calcite)	2.7502	2.2094	2 mm
2 (Quartz)	2.3847	2.4129	3 mm
3 (Ice)	1.7135	1.7161	2 mm

In Figs. 5(a) and 5(b), in terms of the contour of reflected beam intensities, besides the circle at approximately $x_r = 0$ mm, there are still two circular shapes at about $x_r = -3$ mm and $x_r = -4.25$ mm. The intensity circle at approximately $x_r = 0$ mm is directly caused by the reflection of the input interface; meanwhile, the other two circles come from the reflections of the second and the third interfaces between different anisotropic medium layers. It is indicated that the shifts of centers of transmitted intensity profiles in Figs. 5(c) and 5(d) are very distinguishable along the positive x_t axis. Actually, the centers of transmitted intensities are also offset in Figs. 2–4, although the offsets are very small. Based on

the propagation theory of light in media, the shifts are mainly caused by the thickness and the dielectric tensor of the slab. As the thickness of slab increases, the offset becomes greater.

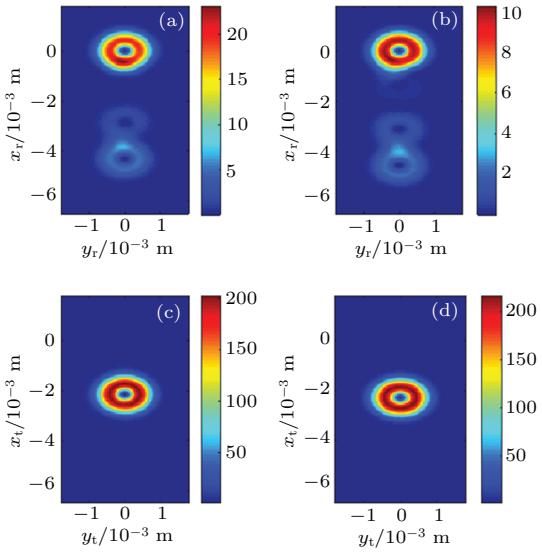


Fig. 5. (color online) Reflected and transmitted beam intensities of LG ($p=0$, $l=1$) beams incident on uniaxial anisotropic three-layered media, showing (a) reflected beam intensities (TE polarized LG beam), (b) reflected beam intensities (TM polarized LG beam), (c) transmitted beam intensities (TE polarized LG beam), and (d) transmitted beam intensities (TM polarized LG beam).

Figures 5(c) and 5(d) show that the contour of transmitted intensities still keeps a circular shape, and the offsets of circular centers are 2.2 mm and 2.3 mm, respectively.

3.2. Discussion on the extension to the general anisotropic multilayered media

In this section, we give a discussion on the extension of the method above to the propagation of LG beam in the general anisotropic multilayered media. The key point is to solve the reflected and transmitted coefficients of the general anisotropic multilayered media. The dielectric tensor ε_j of the j^{th} layer which refers to three arbitrary orthogonal axes, can be written as

$$\varepsilon_j = \begin{bmatrix} \varepsilon_{xx,j} & \varepsilon_{xy,j} & \varepsilon_{xz,j} \\ \varepsilon_{yx,j} & \varepsilon_{yy,j} & \varepsilon_{yz,j} \\ \varepsilon_{zx,j} & \varepsilon_{zy,j} & \varepsilon_{zz,j} \end{bmatrix}. \tag{13}$$

In the 4×4 matrix method,[34] the longitudinal wave vector components $\tilde{k}_{zm,j} = k_{zm,j}/k_0$ $(m=1,2,3,4)$ should be obtained by solving the equation

$$\det(\boldsymbol{\Delta}_j - \widetilde{k}_{z,j}) = 0, \tag{14}$$

where

$$\boldsymbol{\Delta}_j = \begin{bmatrix} \dfrac{\tilde{k}_{x,j}\tilde{\varepsilon}_{zx,j}}{\tilde{\varepsilon}_{zz,j}} & 1-\dfrac{\tilde{k}_{x,j}^2}{\tilde{\varepsilon}_{zz,j}} & \dfrac{\tilde{k}_{x,j}\tilde{\varepsilon}_{zy,j}}{\tilde{\varepsilon}_{zz,j}} & \dfrac{\tilde{k}_{y,j}\tilde{k}_{x,j}}{\tilde{\varepsilon}_{zz,j}} \\ \tilde{\varepsilon}_{xx,j} - \tilde{k}_{y,j}^2 - \dfrac{\tilde{\varepsilon}_{xz,j}}{\tilde{\varepsilon}_{zz,j}}\tilde{\varepsilon}_{zx,j} & \dfrac{-\tilde{k}_{x,j}\tilde{\varepsilon}_{xz,j}}{\tilde{\varepsilon}_{zz,j}} & \tilde{\varepsilon}_{xy,j} - \dfrac{\tilde{\varepsilon}_{xz,j}}{\tilde{\varepsilon}_{zz,j}}\tilde{\varepsilon}_{zy,j} + \tilde{k}_{x,j}\tilde{k}_{y,j} & \dfrac{\tilde{k}_{y,j}\tilde{\varepsilon}_{xz,j}}{\tilde{\varepsilon}_{zz,j}} \\ -\dfrac{\tilde{k}_{y,j}\tilde{\varepsilon}_{zx,j}}{\tilde{\varepsilon}_{zz,j}} & -\dfrac{\tilde{k}_{y,j}\tilde{k}_{x,j}}{\tilde{\varepsilon}_{zz,j}} & -\dfrac{\tilde{k}_{y,j}\tilde{\varepsilon}_{zy,j}}{\tilde{\varepsilon}_{zz,j}} & \dfrac{\tilde{k}_{y,j}^2}{\tilde{\varepsilon}_{zz,j}} - 1 \\ -\tilde{k}_{x,j}\tilde{k}_{y,j} - \tilde{\varepsilon}_{yx,j} + \dfrac{\tilde{\varepsilon}_{yz,j}}{\tilde{\varepsilon}_{zz,j}}\tilde{\varepsilon}_{zx,j} & \dfrac{\tilde{k}_{x,j}\tilde{\varepsilon}_{yz,j}}{\tilde{\varepsilon}_{zz,j}} & \left(\tilde{k}_{x,j}^2 - \tilde{\varepsilon}_{yy,j} + \dfrac{\tilde{\varepsilon}_{yz,j}\tilde{\varepsilon}_{zy,j}}{\tilde{\varepsilon}_{zz,j}}\right) & -\dfrac{\tilde{k}_{y,j}\tilde{\varepsilon}_{yz,j}}{\tilde{\varepsilon}_{zz,j}} \end{bmatrix}. \tag{15}$$

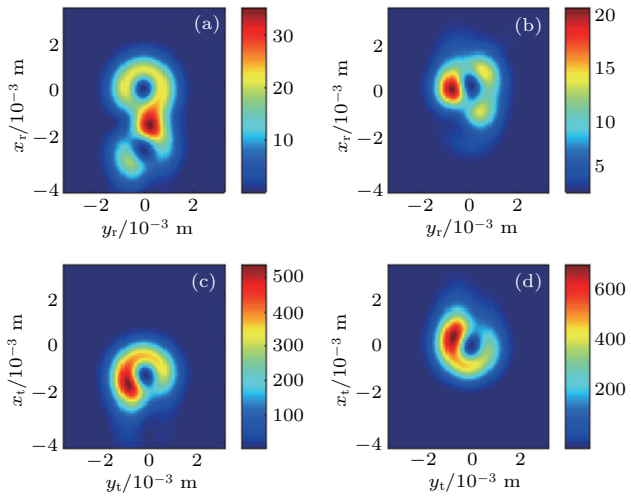


Fig. 6. (color online) Reflected and transmitted beam intensities of LG ($p=0$, $l=1$) beams incident on an anisotropic slab with $h=2$ mm, showing (a) reflected beam intensities (TE polarized LG beam), (b) reflected beam intensities (TM polarized LG beam), (c) transmitted beam intensities (TE polarized LG beam), and (d) transmitted beam intensities (TM polarized LG beam).

Here $\tilde{\varepsilon}_{mn,j} = \varepsilon_{mn,j}/\varepsilon_0$. We can obtain the values of $\widetilde{k}_{zm,j}$ by solving a quartic equation, even though the expression of the root formula is complex. Then with a similar process to that in Section 2, the elements of the matrix $\boldsymbol{T}$ can be obtained. Finally, we can simulate the distributions of reflected and transmitted beam from a general anisotropic multilayered media with the help of Eqs. (5) and (6).

In most cases, we are more concerned about the characteristics of light propagation along the principal axis of the anisotropic media, so we just present numerical results for this case. As is well known, in the principal axis, equation (13) becomes

$$\varepsilon_j = \begin{bmatrix} \varepsilon_{x,j} & 0 & 0 \\ 0 & \varepsilon_{y,j} & 0 \\ 0 & 0 & \varepsilon_{z,j} \end{bmatrix}. \tag{16}$$

Assuming that the principal coordinates of anisotropic media are coincident with the global coordinates, figure 6 presents

the distributions of the reflected and transmitted beam intensities from an anisotropic DAN(4-(N, N-dimethylamino)-3-acetamidonitrobenzene)[24] slab with $\tilde{\varepsilon}_{x,j} = 2.3013$, $\tilde{\varepsilon}_{y,j} = 2.6765$, and $\tilde{\varepsilon}_{z,j} = 2.3966$.

It is shown in Fig. 6 that the distortion of intensity distribution is notable, and the contours cannot keep a full circle, but they still have a hollow shape which is similar to the behavior of incident beam.

4. Conclusions

With the angular spectrum expansion and the 4×4 matrix theory, a method is provided to study the reflection and transmission of LG beams from uniaxial anisotropic multilayered media. An extension of this method to the general anisotropic media is also discussed. The reflected and transmitted beam intensities of the LG beam from a uniaxial anisotropic slab, three-layered uniaxial anisotropic media and a biaxial anisotropic slab are simulated and discussed. It is concluded that for the uniaxial anisotropic slab we used above, the reflected intensity is smaller than the transmitted beam intensity, the distortion of the reflected beam intensity contour is more notable than that of the transmitted beam, and the reflected components for the TM polarized incident beam are smaller than those of the TE polarized case. When the radial index of the incident beam varies from m to n, the contour of intensity distribution will increase (n–m) concentric circles. For three-layered media, the contour of the reflected beam intensities presents three circular rings which are caused by the reflection from the three layers, whereas the contour of the transmitted beam intensities is still one circular ring. Considering the biaxial anisotropic slab, the contours and distributions of the reflected and transmitted beam intensities are greatly influenced by thickness. This work can be applied to the fields of vortex optical information, optical detection, object recognition, and marine remote sensing.

References

[1] Allen L, Beijersbergen M W, Spreeuw R J C and Woerdman J P 1992 *Phys. Rev. A* **45** 8185
[2] Friese M E J, Enger J, Rubinsztein-Dunlop H and Heckenberg N 1996 *Phys. Rev. A* **54** 1593
[3] Nagali E, Sciarrino F, Martini F D, Marrucci L, Piccirillo B, Karimi E and Santamato E 2009 *Phys. Rev. Lett.* **103** 013601
[4] Malik M, O'Sullivan M, Rodenburg B, Mirhosseini M, Leach J, Lavery M P J, Padgett M J and Boyd R W 2012 *Opt. Express* **20** 13195
[5] Foo G, Palacios D M and Swartzlander G A 2005 *Opt. Lett.* **30** 3308
[6] Uribe-Patarroyo N S, Fraine A, Simon D S, Minaeva O and Sergienko A V 2013 *Phys. Rev. Lett.* **110** 043601
[7] Xie T, Zhao S Z, Perrie W, Fang H, Yu W J and He Y J 2016 *Chin. Phys. B* **25** 064101
[8] Xie T, Perrie W, Zhao S Z, Fang H, Yu W J and He Y J 2016 *Chin. Phys. B* **25** 074102
[9] Hui X N, Zheng S L, Chen Y L, Hu Y P, Jin X F, Chi H and Zhang X M 2015 *Sci. Rep.* **5** 10148
[10] Cheng L, Hong W and Hai Z C 2014 *Sci. Rep.* **4** 4814
[11] Karimi E, Piccirillo B, Nagali E, Marrucci L and Santamato E 2009 *Appl. Phys. Lett.* **94** 231124
[12] Karimi E, Schulz S A, Leon I De, Qassim H, Upham J and Boyd R W 2014 *Light: Science and Applications* **3** e167
[13] Ding P F and Pu J X 2011 *Acta Phys. Sin.* **60** 094204 (in Chinese)
[14] Xu Y Q, Zhou G Q and Wang X G 2013 *Chin. Phys. B* **22** 064101
[15] Zhang Y X, Cheng M J, Zhu Y, Gao J, Dan W Y, Hu Z D and Zhao F S 2014 *Opt. Express* **22** 22101
[16] Wang W B, Gozali R, Shi L, Lindwasser L and Alfano R R 2016 *Opt. Lett.* **41** 2069
[17] Aksenov V P and Pogutsa C E 2008 *Quantum Electronics* **38** 343
[18] Lv H and Ke X Z 2009 *Acta Phys. Sin.* **58** 8302 (in Chinese)
[19] Sonoda T and Kozaki S 1989 *Electr. Commun. JPN* **72** 95
[20] Wang M J, Zhang H Y, Liu G S, Li Y L and Dong Q F 2014 *Opt. Express* **22** 3705
[21] Wang Y, Yu K, Zha X, Xu J and Yan J 2006 *Europhys. Lett.* **75** 569
[22] Huang Z X, Xu F, Wang B X, Li M Q and Zhang H Y 2016 *Opt. Commun.* **380** 336
[23] Yu W H, Zhao R H, Deng F, Huang J Y, Chen C D, Yang X B, Zhao Y P and Deng D M 2016 *Chin. Phys. B* **25** 044201
[24] Landry G D and Maldonado T A 1996 *Appl. Opt.* **35** 5870
[25] Tamir T 1986 *J. Opt. Soc. Am. A* **3** 558
[26] Ou J, Jiang Y, Zhang J and He Y 2013 *J. Opt. Soc. Am. A* **30** 2561
[27] Bliokh K Y, Shadrivov I V and Kivshar Y S 2009 *Opt. Lett.* **34** 389
[28] Ni Y and Zhou G 2012 *Opt. Express* **20** 17160
[29] Cincotti G, Ciattoni A and Palma C 2002 *J. Opt. Soc. Am. A* **19** 1680
[30] Ciattoni A, Crosignani B and Porto P Di 2001 *J. Opt. Soc. Am. A* **18** 1656
[31] Chen R P and Wang H T 2010 *Opt. Laser Technol.* **42** 1318
[32] Deng D and Guo Q 2008 *J. Opt. A: Pure Appl. Opt.* **10** 035101
[33] Luo H, Ren Z, Shu W and Wen S 2008 *Phys. Rev. A* **77** 023812
[34] Berreman D W 1972 *J. Opt. Soc. Am.* **62** 502
[35] Wohler H, Haas G, Fritsch M and Mlynski D A 1988 *J. Opt. Soc. Am. A* **5** 1554
[36] Eidner K 1989 *J. Opt. Soc. Am. A* **6** 1657
[37] Lax M, Louisell W H and McKnight W B 1975 *Phys. Rev. A* **11** 1365